

Enhanced infrared absorption of spatially ordered quantum dot arrays

W.Q. Ma ^{*}, Y.W. Sun, X.J. Yang, M. Chong, D.S. Jiang, L.H. Chen

Laboratory of Nano-Optoelectronics, Institute of Semiconductors, Chinese Academy of Sciences, P.O. Box 912, Beijing 100083, PR China

Available online 9 November 2006

Abstract

We have investigated the intersubband absorption for spatially ordered and non-ordered quantum dots (QDs). It is found that the intersubband absorption of spatially ordered QDs is much stronger than that of non-ordered QDs. The enhanced absorption is attributed to the improved size uniformity concurrent with the spatial ordering for the growth condition employed. For the FTIR measurement under normal incidence geometry, using a undoped sample as reference can remove the interference effect due to multiple reflections.

© 2006 Elsevier B.V. All rights reserved.

Keywords: Quantum dots; Spatial ordering; Intersubband absorption

1. Introduction

Quantum dot (QD) infrared photodetector (QDIP) utilizing the intersubband transition may have two advantages comparing with the quantum well counterpart. One is that the intersubband transition is forbidden under normal incidence geometry for an n-type quantum well infrared photodetector (QWIP) while it is allowed for QDIP due to three-dimensional quantum confinement of electrons of the QDs. Therefore, QWIP can operate only by utilizing a light coupling scheme like fabrication of surface gratings, which certainly increases the fabrication cost. Another advantage is that QDIP might work at higher temperature than QWIP due to lower dark current arising from the expected longer lifetime [1,2]. The recently reported value of electron lifetime for intersubband transition for QDs is close to ns [3] while that is typically ps for quantum well structure [4]. However, the bottleneck to enhance performance of QDIP is the large size fluctuation and relatively low density of the present self-assembled QDs [5]; also the intersubband absorption of QDs under normal incidence geometry is still very low due to the disk-like shape of QDs, i.e., the height of the QDs is much smaller than

the width. To overcome these drawbacks, many design and growth schemes have been proposed. For example, QD density is found to increase significantly by growing InAs QDs on an AlAs layer resulting in an enhanced performance of the QDIP [6]; QDIP signal under normal incidence geometry increases significantly by employing the wave function coupled QDs into the photodetector structure compared to the decoupled QDs [7].

This work investigates the intersubband absorption of spatially ordered QDs. Although, for photodetector application, the QDs may not need to be spatially ordered, we do find that the absorption of ordered QDs is much stronger than that of non-ordered QDs for normal incident light. The ordered QDs are vertically correlated and laterally ordered. The enhanced absorption is attributed to that, for the growth condition employed, the spatial ordering is concurrent with an improved size ordering. The absorption peak is located at about 11 μm . The samples were also polished at 45° at the two edges and the corresponding absorption was measured at waveguide geometry, which again confirms that ordered dots demonstrate much stronger absorption.

2. Sample growth

For the absorption measurements, two samples were grown on semi-insulating GaAs (100) substrates. The

^{*} Corresponding author.

E-mail address: wqma@semi.ac.cn (W.Q. Ma).

structure consists of 1 μm thick GaAs buffer layer by Si doped to $1 \times 10^{18} \text{ cm}^{-3}$, 20 periods of $\text{In}_{0.53}\text{Ga}_{0.47}\text{As}$ (2.5 nm)/GaAs (20 nm) multilayers followed by a 0.5 μm thick GaAs layer by Si doped to $1 \times 10^{18} \text{ cm}^{-3}$. The (In,Ga)As layer was doped by Si to $5 \times 10^{17} \text{ cm}^{-3}$ to generate electrons. The (In,Ga)As/GaAs multilayer was grown at 540 $^{\circ}\text{C}$ for the first sample, denoted as sample *a*, while that was grown at 480 $^{\circ}\text{C}$ for the second sample denoted as sample *b*. The growth rate of GaAs and InAs is 0.24 and 0.27 ML/s, respectively. The two samples were grown by using As_2 realized by setting the As cracking zone temperature at 850 $^{\circ}\text{C}$ and base zone temperature at 380 $^{\circ}\text{C}$. The whole growth procedure was monitored *in situ* by reflection high-energy electron diffraction (RHEED). The RHEED pattern changes from streaky to spotty for the two samples after about 70% (In,Ga)As layer or about 6 ML deposition indicating appearance of three-dimensional islands. For the morphological investigation discussed below by atomic force microscopy (AFM), another two 15-period stacked QD samples without the GaAs top layer were grown at the same condition as samples *a* and *b*, respectively.

3. AFM and PL characterizations

Fig. 1a and b show the AFM images of the (In,Ga)As layer after 15-period stacking for samples *a* and *b*, respectively. It can be seen that the QDs demonstrate a distinct lateral ordering for sample *a* while no lateral ordering is observed for sample *b*. This conclusion is confirmed by the image of the two-dimensional (2D) fast Fourier transformation (FFT) shown in the inset of Fig. 1a. The only difference of the growth condition between samples *a* and *b* is that sample *a* was grown at 540 $^{\circ}\text{C}$ while sample *b* at 480 $^{\circ}\text{C}$. Actually, for a vertically correlated system, the observed lateral ordering is in general attributed to the enhanced surface diffusion and the vertical transfer of corresponding anisotropic strain pattern due to the anisotropy of surface diffusion [8]. That is, in order to generate the lateral ordering, the migration length of the adatoms should be large enough to respond to the underlying strain distri-

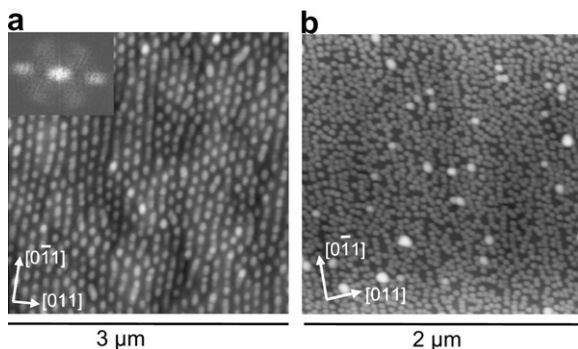


Fig. 1. AFM top views of the ordered (a) and non-ordered QDs (b) after 15-period stacking. The inset of (a) shows the FFT image. The scanning range is $3 \times 3 \mu\text{m}^2$ and $2 \times 2 \mu\text{m}^2$ for (a) and (b), respectively.

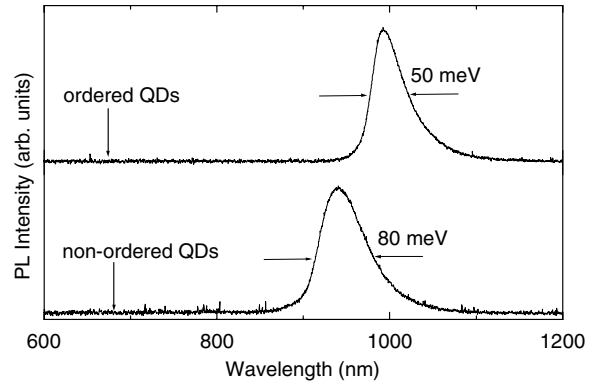


Fig. 2. PL spectra of ordered dots and non-ordered dots measured at room temperature.

bution in a short enough time. Therefore, the lateral ordering is not observed for the sample grown at 480 $^{\circ}\text{C}$ due to much smaller migration length of the adatoms compared to the sample grown at 540 $^{\circ}\text{C}$. As shown in the inset of Fig. 1a, the QDs are laterally aligned in a hexagonal way while in Ref. [8] the linear chains of QDs are revealed. Such a difference may be due to the fact that the sample *a* was grown under As_2 pressure while the linear chains reported in Ref. [8] were grown under As_4 atmosphere. The lateral island–island interaction energy is minimum for the hexagonal arrangements of QDs. However, realization of the hexagonal ordering not only depends on the growth energetics but also is related to a delicate growth kinetics. The detailed study on the formation of the hexagonal ordering of QDs is beyond the scope of this paper [9].

Fig. 2 depicts the photoluminescence (PL) spectra of samples *a* and *b* measured at room temperature. The full width at half maximum (FWHM) of the PL spectrum is 50 and 80 meV for samples *a* and *b*, respectively. This indicates that, for the growth condition employed, an enhanced lateral ordering of QDs is also concurrent with an enhanced size ordering. The red shift of the PL peak of sample *a* compared to sample *b* is because sample *a* was grown at higher temperature which correspondingly results in a larger size of QDs. From Fig. 1a and b, it can be seen clearly that the QD size of sample *a* is larger than that of sample *b*. Therefore, the measured PL peak positions of the two samples are in agreement with the AFM results.

4. FTIR measurements and the discussion

For the absorption measurements under normal incidence geometry by Fourier transform infrared (FTIR) spectrometer, in order to remove the interference effect due to the multiple reflections at interfaces, we grew another two samples, denoted as samples *a'* and *b'*, corresponding to samples *a* and *b*, respectively [10]. For each of them, the only difference is that the (In,Ga)As layer is not doped while the other parameters and the growth condition are exactly the same as the corresponding doped photodetector sample. The solid and dotted lines in Fig. 3 show the

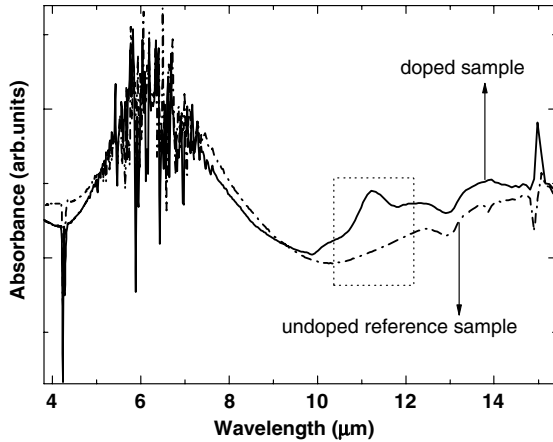


Fig. 3. Room temperature FTIR spectra under normal incidence geometry using air as reference for samples *a* and *a'*.

FTIR absorption spectra of samples *a* and *a'* by using air as reference measured at room temperature. The disordered sharp peaks around 5–7 μm in Fig. 3 is due to the non-reproducibility of the measurement environment of air. Because there should be no absorption for the undoped sample, the observed peaks of the dotted line in Fig. 3 are assumed to be due to the interference. However, for the doped sample, the measured FTIR spectrum should be the real absorption signal superimposed on the interference fringes. In order to unravel the real absorption signal, we performed FTIR measurements for samples *a* and *b* by using the corresponding undoped samples as references. The results are shown in Fig. 4. For sample *a*, we detected a peak at around 11 μm while no clear normal incidence absorption peak was detected for sample *b*. To test if the FTIR measurement method for normal incidence geometry is correct, we cut samples *a* and *b* in the same length and width and polished the cut piece 45° at the two edges and performed the FTIR under the waveguide geometry still at room temperature and the results are shown in Fig. 5. For sample *a*, still an absorption peak located around

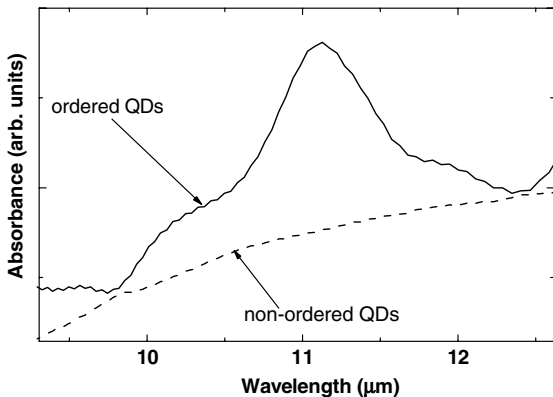


Fig. 4. Room temperature FTIR spectra under normal incidence geometry using the corresponding undoped sample as reference.

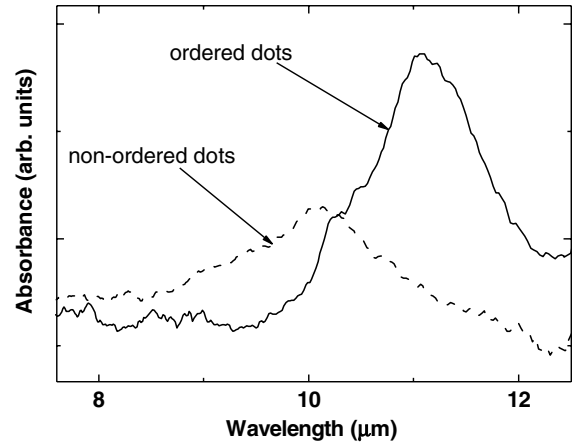


Fig. 5. Room temperature FTIR spectra under waveguide geometry.

11 μm was detected while for sample *b* a peak around 10 μm was also detected. However, the absorption signal of sample *a* is about four times stronger than that of sample *b*. The fact that for sample *b* the absorption is observed for waveguide geometry while not for normal incidence geometry may indicate that the absorption efficiency under the normal incidence geometry is very low. We think that the enhanced absorption of the ordered QD sample is due to the improved size uniformity as supported by the PL results shown in Fig. 2. The inhomogeneous broadening can weaken the absorption since, to reach the same level of absorption, more number of QDs are required to compensate the loss due to the size fluctuation.

5. Conclusions

In summary, we find that the intersubband absorption of spatially ordered QDs is much stronger than that of non-ordered QDs. The enhanced absorption is attributed to the improved size uniformity concurrent with the spatial ordering for the growth condition employed. For the FTIR measurement under normal incidence geometry, using an undoped sample as reference can remove the interference effect due to multiple reflections.

Acknowledgement

This work is supported by Research Grant No. HT3Y83582005.

References

- [1] M.A. Kinch, J. Electron. Mater. 29 (2000) 809.
- [2] M.A. Kinch, A. Yariv, Appl. Phys. Lett. 55 (1989) 2093.
- [3] J. Urayama, T. Norris, J. Singh, P. Bhattacharya, Phys. Rev. Lett. 86 (2001) 4930.
- [4] H.C. Liu, in: H. Liu, F. Capasso (Eds.), Intersubband Transitions in Quantum Wells: Physics and Device Applications I, Academic Press, San Diego, 2000.

- [5] J. Phillips, *J. Appl. Phys.* 91 (2002) 4590.
- [6] S. Chakrabarti, D. Stiff-Roberts, X.H. Su, P. Bhattacharya, G. Ariyawansa, A.G.U. Perera, *J. Phys. D: Appl. Phys.* 38 (2005) 2135.
- [7] A. Adawi, E.A. Zibik, L.R. Wilson, A. Lemaitre, J.W. Cockburn, M. Hopkinson, G. Hill, S.L. Liew, A.G. Cullis, *Appl. Phys. Lett.* 82 (2003) 3415.
- [8] W.Q. Ma, M.L. Hussein, J.L. Shultz, G.J. Salamo, T.D. Mishima, M.B. Johnson, *Phys. Rev. B* 69 (2004) 233312.
- [9] W.Q. Ma, Y.W. Sun, X.J. Yang, D.S. Jiang, L.H. Chen, unpublished.
- [10] M. Hussein, W.Q. Ma, G.J. Salamo, *Mater. Res. Soc. Symp. Proc.* 776 (2003) Q11.29.1.